

Article

Astaxanthin Activates Nuclear Factor Erythroid-Related Factor 2 and the Antioxidant Responsive Element (Nrf2-ARE) Pathway in the Brain after Subarachnoid Hemorrhage in Rats and Attenuates Early Brain Injury

Qi Wu ¹, Xiang-Sheng Zhang ¹, Han-Dong Wang ^{1,*}, Xin Zhang ^{1,*}, Qing Yu ², Wei Li ¹, Meng-Liang Zhou ¹ and Xiao-Liang Wang ¹

¹ Department of Neurosurgery, Jinling Hospital, School of Medicine, Nanjing University, Nanjing 210002, China; E-Mails: 18652021010@163.com (Q.W.); zhangxssp@163.com (X.-S.Z.); lwxzlw@gmail.com (W.L.); mlzhou1979@hotmail.com (M.-L.Z.); wangxiaoliang1234@hotmail.com (X.-L.W.)

² Department of Clinical Laboratory, Affiliated Hospital of Nanjing University of Chinese Medicine, Nanjing 210029, China; E-Mail: njyuqing@me.com

* Authors to whom correspondence should be addressed; E-Mails: njhdwang@hotmail.com (H.-D.W.); njzx@smail.nju.edu.cn (X.Z.); Tel.: +86-25-8086-0071 (H.-D.W.); +86-25-8086-3401 (X.Z.); Fax: +86-25-8481-7581 (H.-D.W.); +86-25-5180-5396 (X.Z.).

External Editor: Keith B. Glaser

Received: 9 October 2014; in revised form: 19 November 2014 / Accepted: 8 December 2014 /

Published: 18 December 2014

Abstract: Astaxanthin (ATX) has been proven to ameliorate early brain injury (EBI) after experimental subarachnoid hemorrhage (SAH) by modulating cerebral oxidative stress. This study was performed to assess the effect of ATX on the Nrf2-ARE pathway and to explore the underlying molecular mechanisms of antioxidant properties of ATX in EBI after SAH. A total of 96 male SD rats were randomly divided into four groups. Autologous blood was injected into the prechiasmatic cistern of the rat to induce an experimental SAH model. Rats in each group were sacrificed at 24 h after SAH. Expressions of Nrf2 and heme oxygenase-1 (HO-1) were measured by Western blot and immunohistochemistry analysis. The mRNA levels of HO-1, NAD (P) H: quinone oxidoreductase 1 (NQO-1), and glutathione S-transferase- α 1 (GST- α 1) were determined by real-time polymerase chain reaction (PCR). It was observed that administration of ATX post-SAH could up-regulate the cortical expression of these agents, mediated in the Nrf2-ARE pathway at both pretranscriptional and posttranscriptional

levels. Meanwhile, oxidative damage was reduced. Furthermore, ATX treatment significantly attenuated brain edema, blood–brain barrier (BBB) disruption, cellular apoptosis, and neurological dysfunction in SAH models. This study demonstrated that ATX treatment alleviated EBI in SAH model, possibly through activating the Nrf2-ARE pathway by inducing antioxidant and detoxifying enzymes.

Keywords: astaxanthin; early brain injury; subarachnoid hemorrhage; nuclear factor erythroid-related factor 2

1. Introduction

Astaxanthin (ATX) is a carotenoid widely found in algae and aquatic animals, which has powerful antioxidant activity [1]. Previous studies have revealed that ATX, with its antioxidative property, is beneficial as a therapeutic agent for various diseases both *in vivo* and *in vitro* without any side effects or toxicity [2–4]. Our earlier research has demonstrated that ATX administration after subarachnoid hemorrhage (SAH) can up-regulate the cortical endogenous antioxidant agents and prevent oxidative damage in experimental SAH models, thus alleviating early brain injury (EBI) [5], which is considered the most common cause of disability and death in SAH patients [6]. To date, however, there are few studies concerning the underlying molecular mechanisms of ATX in the SAH model.

Nrf2 is a basic leucine zipper redox-sensitive transcription factor, which transfers from the cytoplasm to the nucleus and binds to the ARE to activate transcription of several antioxidant genes under conditions of oxidative or xenobiotic stress [7–9]. The Nrf2-ARE pathway has been proven to play a beneficial role in EBI after SAH, possibly through inducing antioxidant and detoxifying enzymes to reduce cerebral oxidative stress [10].

In the previous studies concerning ATX and the Nrf2-ARE pathway, effects of ATX on Nrf2-ARE pathway activation had been investigated *in vivo* and *in vitro* models [1,11]. Tripathi and Jena [1] provided the evidence that ATX up-regulated the levels of Nrf2 and phase-II enzymes to exert its protective effects against cyclophosphamide-induced oxidative stress in rat liver. Zhang *et al.* [11] found that ATX could up-regulate the expression of Nrf2 in leukemia K562 cells in time- and dose-dependent manners. Previous studies had evaluated the activation of the Nrf2-ARE pathway, always using ATX as a pretreatment. However, there is no study investigating the effect of ATX on the Nrf2-ARE pathway in SAH. Thus, the purpose of this study was to explore whether ATX treatment post SAH could activate the Nrf2-ARE pathway and ameliorate EBI in the SAH model.

2. Results

2.1. General Observation

There were no significant differences detected in body weight, temperature, or injected arterial blood gas data among the groups.

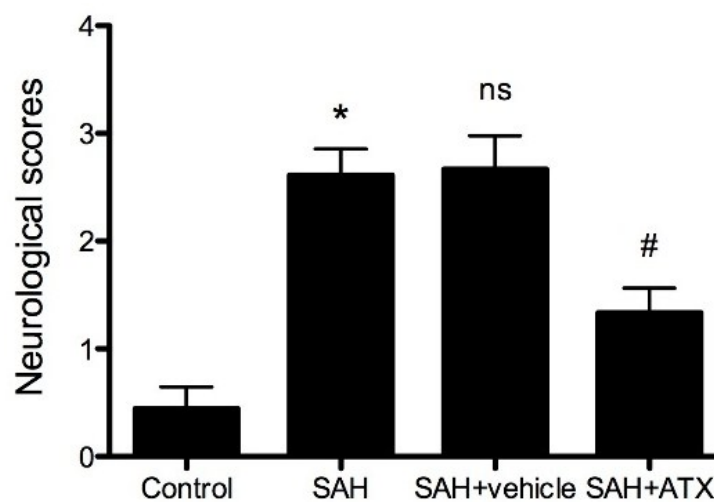
2.2. Neurological Scores

An independent investigator blinded to the experimental groups and carried out a battery of tests looking at appetite, activity, and neurological deficits [12] before the rats were sacrificed. The deficits were scored with the scoring system shown in Table 1. Compared to the control group, neurological impairment caused by SAH was remarkable in the SAH group (Figure 1, $p < 0.001$). The SAH + ATX group showed better performance than either the SAH group or the SAH + vehicle group at 24 h after SAH, and the difference was statistically significant (Figure 1, $p < 0.05$). There were no significant differences between the SAH group and SAH + vehicle group (Table 1, $p > 0.05$).

Table 1. Behavior and activity scores.

Category	Behavior	Score
Appetite	Finished meal	0
	Left meal unfinished	1
	Scarcely ate	2
Activity	Walked and reached at least three corners of the cage	0
	Walked with some stimulation	1
	Almost always lying down	2
Deficits	No deficits	0
	Unstable walk	1
	Impossible to walk	2

Figure 1. Neurological scores of each group. Data are expressed as means \pm SEM. Neurologic impairments of rats due to SAH were improved because of the administration of Astaxanthin (ATX) after SAH. * $p < 0.0001$, compared with control group; # $p < 0.05$ compared with SAH group and SAH + vehicle group, respectively; ^{ns} $p > 0.05$, compared with SAH group.

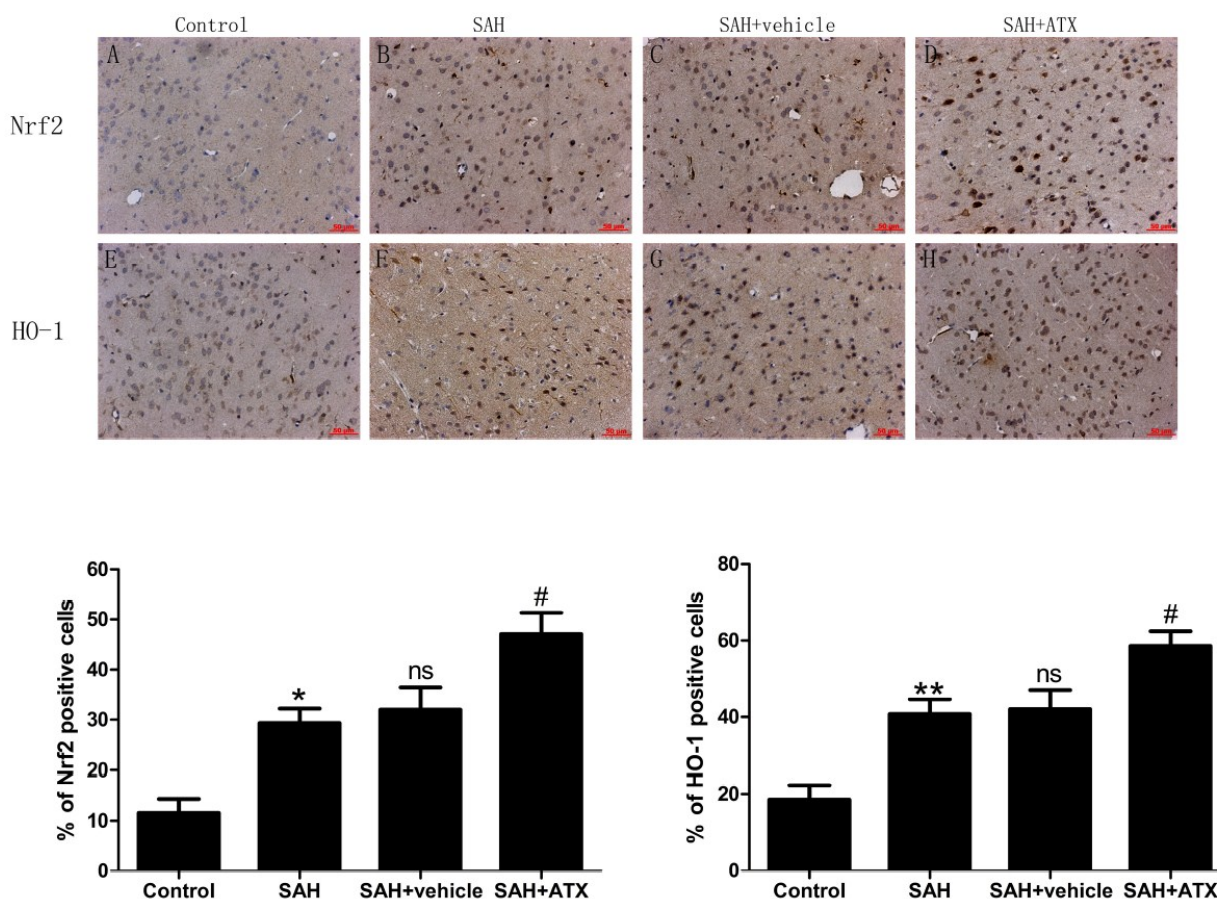


2.3. Immunohistochemistry for Nrf2 and HO-1 Expression

As is shown in Figure 2, a few Nrf2 and HO-1 positive cells stained brown and could be observed in the cortex of the control group. More Nrf2 and HO-1 positively immunostained cells were found in the

SAH group and the SAH + vehicle group. In the SAH + ATX group, the number of Nrf2 and HO-1 positive cells was further increased compared with the SAH group or SAH + vehicle group.

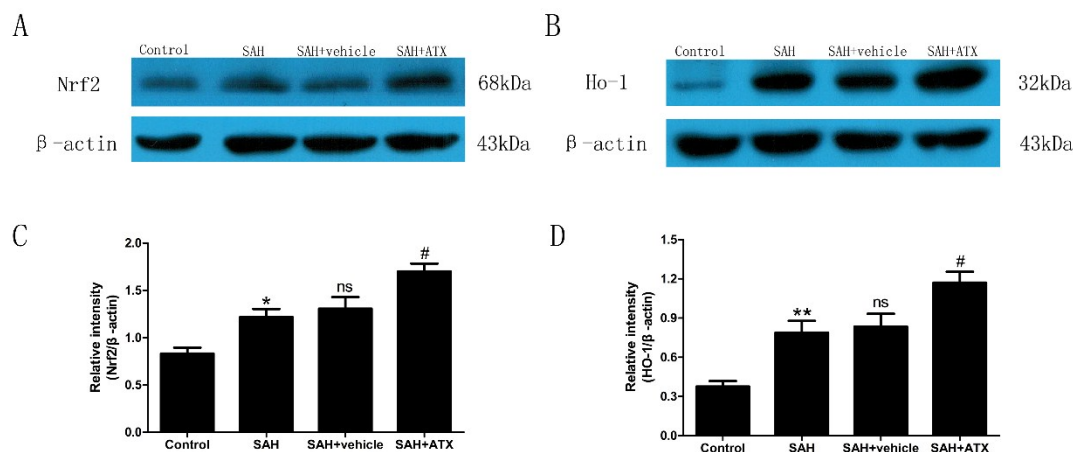
Figure 2. Representative photomicrographs showing Nrf2 (A–D) and HO-1 (E–H) immunohistochemistry staining of the temporal lobe in the experimental groups. As shown, a few Nrf2 and HO-1 stained cells were observed in the control group ($n = 6$), whereas numerous Nrf2 and HO-1 stained cells could be seen in the SAH group ($n = 6$) and SAH + vehicle group ($n = 6$). After ATX administration ($n = 6$), the immune-positive cells of Nrf2 and HO-1 in the cortex further increased following SAH. (I) Quantification analysis of immune reactive cells for Nrf2 and HO-1. The administration of ATX could induce Nrf2 and Nrf2-ARE pathway-related agent activation. Data are expressed as means \pm SEM. * $p < 0.05$ compared with control group; ** $p < 0.01$ vs. control group; # $p < 0.05$ vs. SAH group and SAH + vehicle group, respectively; ^{ns} $p > 0.05$ vs. SAH group.



2.4. Western Blot Analysis for Nrf2 and HO-1 Expression

As is shown in Figure 3, low levels of Nrf2 and HO-1 were expressed in the control group. The levels of Nrf2 and HO-1 were significantly increased in the SAH and SAH + vehicle groups compared with the control group ($p < 0.05$ and $p < 0.01$, respectively) at 24 h after SAH. There was no significant difference between the SAH and the SAH + vehicle groups ($p > 0.05$) (Figure 3). After ATX treatment, the increased expression of Nrf2 and HO-1 was remarkable compared with that in the SAH group ($p < 0.05$) (Figure 3).

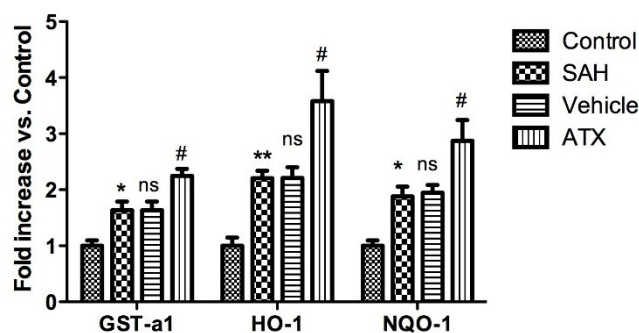
Figure 3. Representative autoradiogram of the Nrf2 (A) and HO-1 (B) in the experimental groups, and quantitative analysis of the Western blot results for Nrf2 (C) and HO-1 (D). SAH could induce a significant increase of Nrf2 and HO-1 expression in the rat cortex samples compared with the control group. After ATX administration, the protein levels of Nrf2 and HO-1 were further up-regulated. Data are expressed as means \pm SEM. * $p < 0.05$ compared with control group; ** $p < 0.01$ vs. control group; # $p < 0.05$ vs. SAH and SAH + vehicle group, respectively; ^{ns} $p > 0.05$ vs. SAH group.



2.5. Quantitative Real-Time Polymerase Chain Reaction (PCR)

The cortical mRNA levels of HO-1, NQO1, and GST- α 1 were significantly increased in the SAH and SAH + vehicle groups as compared with the control group ($p < 0.01$, $p < 0.05$ and $p < 0.05$, respectively). There are no significant differences in mRNA expressions of HO-1, NQO1, and GST- α 1 between the SAH and SAH + vehicle groups ($p > 0.05$). The mRNA expressions of HO-1, NQO1, and GST- α 1 in the cortex in the SAH + ATX group were markedly higher up-regulated than those in the SAH or SAH + vehicle group ($p < 0.05$) (Figure 4).

Figure 4. The cortical mRNA expressions of HO-1, NQO1, and GST- α 1 in the control group ($n = 6$), SAH group ($n = 6$), SAH + vehicle group ($n = 6$), and SAH + ATX group ($n = 6$). SAH could induce a marked increase in HO-1, NQO1, and GST- α 1 mRNA expressions in the rat cortex compared with the control group. After ATX administration, the mRNA expressions of Nrf2-ARE pathway-related agents were significantly up-regulated. * $p < 0.05$ vs. control group; ** $p < 0.01$ vs. control group; # $p < 0.05$ vs. SAH group and SAH + vehicle group, respectively; ^{ns} $P > 0.05$ vs. SAH group.



2.6. Enzyme Activity Assay for NQO1 and GST- α 1

Compared with the control group, enzyme activities of NQO1 and GST- α 1 were up-regulated after SAH ($p < 0.05$) (Figure 5). On the other hand, ATX administration after SAH significantly increased NQO1 and GST- α 1 activity in rat cortex. There was a significant difference between the SAH + ATX and the other groups (Figure 5).

Figure 5. NQO1 (A) and GST- α 1 (B) enzyme activities in the cortex in the control group ($n = 6$), the SAH group ($n = 6$), the SAH + vehicle group ($n = 6$), and the SAH + ATX group ($n = 6$). SAH could significantly elevate the activities of NQO1 and GST- α 1. In the SAH + ATX group, the activities of NQO1 and GST- α 1 were significantly up-regulated compared with the SAH + vehicle group. * $p < 0.05$ vs. control group; # $p < 0.05$ and ## $p < 0.01$ vs. SAH + vehicle group; ns $p > 0.05$ compared with the SAH group.

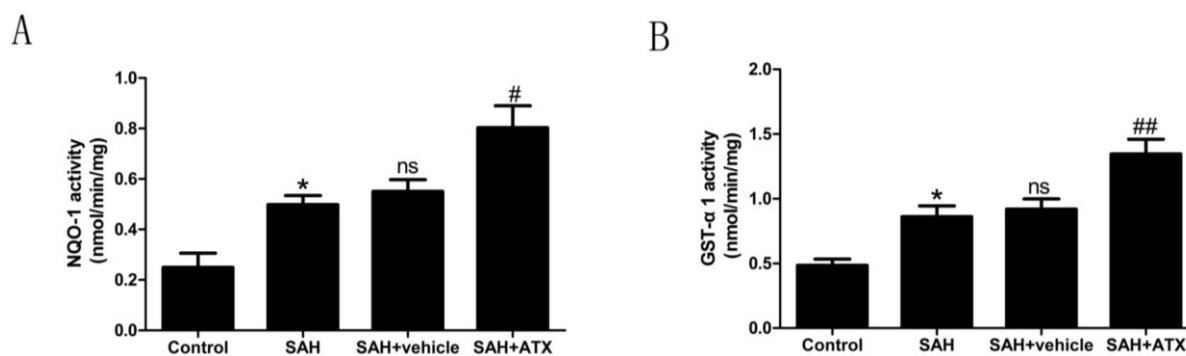
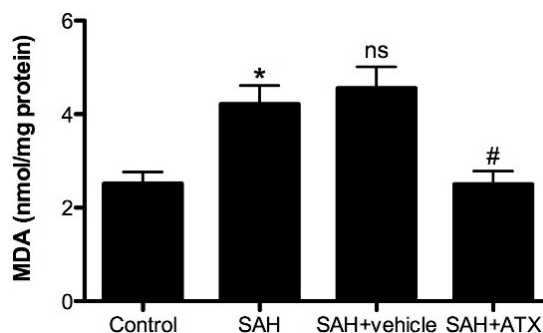


Figure 6. Malondialdehyde (MDA) levels in the control group ($n = 6$), SAH group ($n = 6$), SAH + vehicle group ($n = 6$), and SAH + ATX group ($n = 6$). As shown, the level of MDA in the cortex increased remarkably at 24 h after SAH. ATX treatment significantly suppressed the production of MDA after SAH. The values are expressed as mean \pm SEM. * $p < 0.05$ compared with control group; # $p < 0.05$ compared with SAH group and SAH + vehicle group, respectively. ns $p > 0.05$ vs. SAH group.



2.7. Malondialdehyde (MDA) Levels

Malondialdehyde (MDA) is the end product of lipid peroxidation of polyunsaturated fatty acids in cellular membranes. MDA has been identified as a reliable marker of oxidative stress, which can represent cell damages indirectly. As shown in Figure 6, a significant increase in MDA levels was detected in the cortex samples at 24 h after SAH as opposed to the control group ($p < 0.05$). The level of MDA was

significantly decreased with ATX treatment compared with the SAH and SAH + vehicle groups ($p < 0.05$, respectively).

2.8. Brain Water Content

Brain edema is a major cause of poor outcome after SAH. Blood-brain barrier (BBB) disruption was considered to be one of the most important pathogeneses resulting in brain edema [13]. In the present study, brain water content increased significantly at 24 h after SAH as compared with the control group ($p < 0.01$) (Figure 7). It was observed that ATX treatment significantly reduced brain edema as compared with the SAH and SAH + vehicle groups ($p < 0.05$, respectively) (Figure 7).

Figure 7. Percentages of brain water content in the control group ($n = 6$), SAH group ($n = 6$), SAH + vehicle group ($n = 6$), and SAH + ATX group ($n = 6$). As shown, the brain water content increased remarkably at 24 h after SAH. ATX treatment reduced brain water content significantly compared with the SAH group or SAH + vehicle group. The values are expressed as mean \pm SEM. ** $p < 0.01$ compared with control group; # $p < 0.05$ compared with SAH group and SAH + vehicle group, respectively. ^{ns} $p > 0.05$ vs. SAH group.

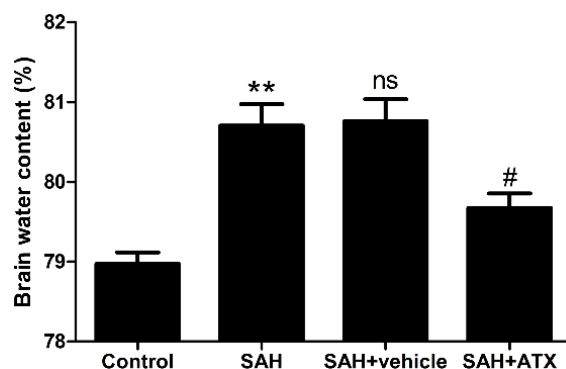
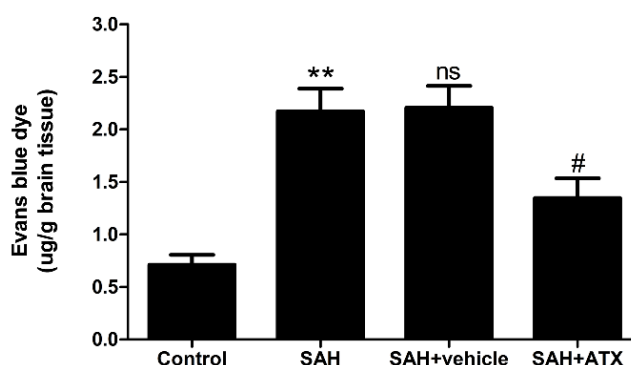


Figure 8. Evans blue (EB) extravasations in control the group ($n = 6$), SAH group ($n = 6$), SAH + vehicle group ($n = 6$), and SAH + ATX group ($n = 6$). SAH induced a significant increase in blood-brain barrier extravasation in the cortex compared with the control group, and ATX administration significantly decreased EB extravasation in this group compared with the SAH group or SAH + vehicle group. The values are expressed as mean \pm SEM. ** $p < 0.01$ compared with control group; # $p < 0.05$ compared with SAH group and SAH + vehicle group, respectively; ^{ns} $p > 0.05$ vs. SAH group.



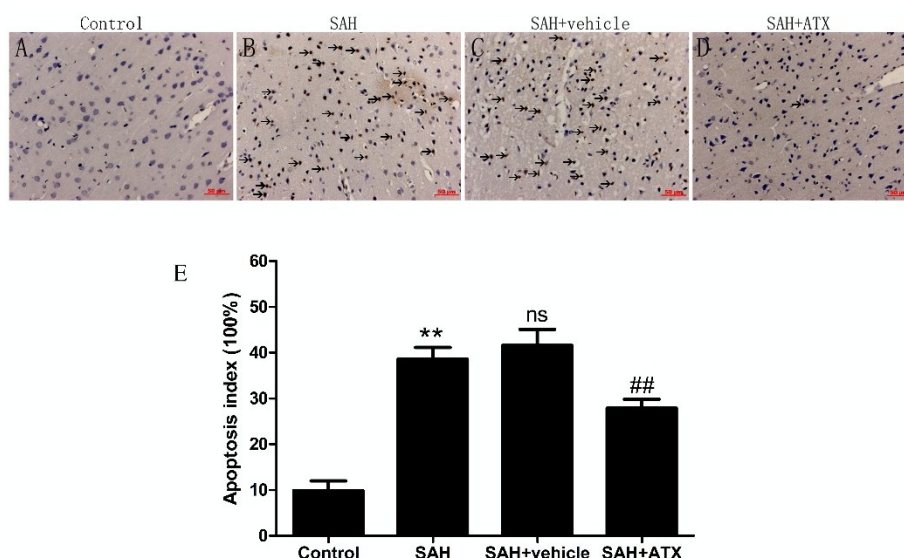
2.9. Blood-Brain Barrier Permeability

Evans blue (EB) extravasation as an indicator of BBB permeability was measured at 24 h after SAH, which is illustrated in Figure 8. The SAH group and SAH + vehicle group showed a significant increase of EB extravasation when compared with the control group ($p < 0.01$). As shown in Figure 8, ATX treatment significantly inhibited EB extravasation ($p < 0.05$), attenuating BBB permeability after SAH.

2.10. Terminal Deoxynucleotidyl Transferase-Mediate dUTP Nick end Labeling Staining (TUNEL) Assay

As illustrated in Figure 9, a few terminal deoxynucleotidyl transferase-mediate dUTP nick end labeling (TUNEL)-positive cells were found in the control group (Figure 9A). Compared with the control group, the percentages of apoptosis cells in the cortex significantly increased in the SAH and SAH + vehicle groups ($p < 0.01$) (Figure 9B,C). In the SAH + ATX group, the apoptosis index significantly decreased ($p < 0.01$) (Figure 9D) when compared with SAH and SAH + vehicle groups.

Figure 9. Representative photomicrographs of terminal deoxynucleotidyl transferase-mediate dUTP nick end labeling (TUNEL) staining (scar bar, 50 μm) and the apoptosis index of the cortex in the control group ($n = 6$), SAH group ($n = 6$), SAH + vehicle group ($n = 6$), and SAH + ATX group ($n = 6$). Control group (A) showing few apoptotic cells in the cortex. More TUNEL staining cells with the nucleus stained brown (arrows) could be observed in the SAH and SAH + vehicle groups (B,C). The proportion of apoptotic cells decreased significantly in the ATX group (D). (E) Apoptosis index. Bars represent the mean \pm SEM. ** $p < 0.01$ vs. control group, ## $p < 0.01$ vs. SAH + vehicle group, ns $p > 0.05$ vs. SAH group.



3. Discussion

The present study demonstrated that ATX activated the Nrf2-ARE pathway to up-regulate the expression of Nrf2-regulated enzymes against oxidative stress, such as HO-1, NQO1 and GST- α 1, at 24 h after SAH. Accordingly, oxidative damage in the cortex induced by SAH was reduced. In the

meantime, ATX administration attenuated brain edema, BBB disruption, cellular apoptosis, and neurological dysfunction in SAH models.

EBI is an important cause of high morbidity and mortality in patients suffering from SAH [14]. The exact mechanism of EBI remains obscure, although it is probably due to the elevation of intracranial pressure, cerebral perfusion disruption, brain edema, BBB breakdown, and neuronal cell death [12]. Accumulating evidence has demonstrated that oxidative stress plays an important role in the pathogenesis of EBI [15]. It has been reported that excessive reactive oxygen species (ROS) and reactive nitrogen species (RNS) including hydroxyl radical, superoxide anion, hydrogen peroxide, nitric oxide, and peroxynitrite are generated in the early period after SAH, consuming enzymatic and non-enzymatic antioxidant defense systems [16]. Moreover, these free radicals will promote lipid peroxidation, protein breakdown, and DNA damage, resulting in neuronal damage, cellular apoptosis, endothelial injury, and BBB disruption [15]. It may be a novel therapeutic target of SAH.

ATX is a carotenoid containing an additional carboxyl group on each ring structure at the two extremities. It is a more effective antioxidant than vitamin E, by 100–1000 times. [17]. In addition, it has been reported that ATX possesses a variety of pharmacological properties without any side effects or toxicity, including anti-inflammatory, immunomodulatory, and anti-tumor activities [4,18,19]. Previous studies have proven that ATX plays a protective role in models of cardiovascular diseases including myocardial ischemia and reperfusion [20,21]. In a recent study, Shen *et al.* [2] demonstrated that ATX could reduce ischemia-related injury in brain tissue through inhibition of oxidative stress, reduction of glutamate release, and anti-apoptosis. Nevertheless, limited research has investigated the protective effect of ATX in SAH. Our previous study has proven that ATX treatment significantly attenuates brain edema and BBB disruption, reduces cellular apoptosis, and improves neurologic function at 24 h after SAH [5]. However, further studies should be performed to explore the underlying signaling pathway between ATX and SAH.

Increasing data indicate that Nrf2 plays a key role in antioxidant protection, which was revealed in various central nervous system diseases, such as cerebral ischemia, traumatic brain injury, and SAH [8,10,22,23]. Under these pathological conditions, Nrf2 translocates into the nucleus and then binds to ARE, transactivating a group of cytoprotective enzymes to protect cells against oxidative and xenobiotic damage. The protective effects of ATX on the Nrf2-ARE pathway activation in certain diseases have been demonstrated in previous studies [1,11,24]. Therefore, we hypothesized that ATX could also activate the Nrf2-ARE pathway in brain after SAH to alleviate EBI through inhibition of oxidative stress secondary to the up-regulation of antioxidant enzymes. In the present study, we found that SAH induced a significant increase in Nrf2 protein levels in the cortex. The mRNA levels of Nrf2-regulated gene products, HO-1, NQO1, and GST- α 1, were also up-regulated at 24 h after SAH. This suggested triggering of the Nrf2-ARE pathway in the brain after SAH to exert antioxidant and detoxifying properties. Compared with SAH and SAH + vehicle groups, ATX administration significantly increased the Nrf2 protein level, up-regulated the expression of HO-1, NQO1 and GST- α 1 at both pretranscriptional and posttranscriptional levels. HO-1, NQO1, and GST- α 1 are potent antioxidant and detoxifying enzymes. HO-1 could reduce ROS production via generating biliverdin or bilirubin. NQO1 is able to protect cells against the adverse effects of quinones and related compounds. Unlike these two enzymes, GST- α 1 performs the protective effect by up-regulating the content of endogenous glutathione [25,26]. Accordingly, ATX administration reduced the oxidant damage and ameliorated the EBI in the SAH models in this study.

However, the mechanism of activation of the Nrf2-ARE pathway by ATX has not been completely elucidated. Several kinases, such as phosphoinositol-3 kinase (PI3K) and extra cellular signal-regulated protein kinase (ERK) have been reported to activate Nrf2 in response to some stimuli [27,28]. On the other hand, it has been reported that ATX induces activation of PI3K and ERK under some conditions [29,30]. It may be part of the mechanisms involved in the activation of the Nrf2-ARE pathway by ATX after SAH, which needs to be investigated in further studies.

In this study, we used the prechiasmatic cistern SAH model that is appropriate for EBI research since it produces similar pathological and pathophysiological processes to that in human with an acceptable mortality rate [31,32]. However, our study has several limitations. Firstly, ATX treatment was conducted only once and we do not know whether multiple treatments with different time courses would be effective. In addition, ATX may have other protective effects against EBI after SAH that were not evaluated in this study, such as anti-inflammatory and immunomodulatory properties. Lastly, Nrf2 knockout mice were not used in this research, although the improved outcome was regarded partly by beneficial effects of ATX through activating the Nrf2-ARE pathway. Therefore, comprehensive studies are still warranted.

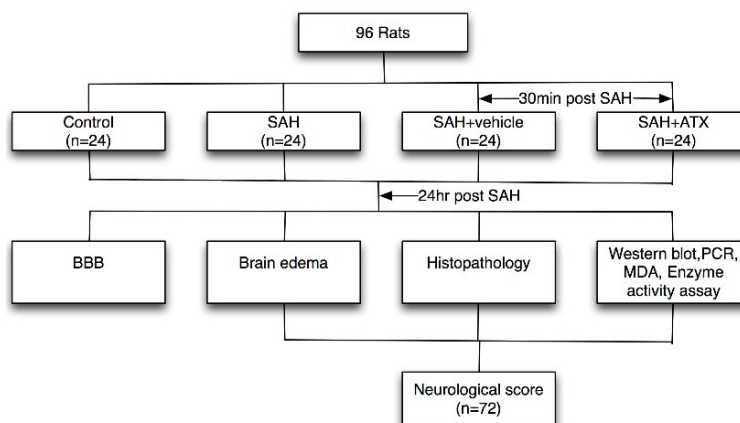
4. Experimental Section

4.1. Animals

Male Sprague-Dawley rats (250–300 g) were purchased from the Animal Center of Jinling Hospital, Nanjing, China. They were acclimated in a humidified room and maintained on a standard pellet diet at the Animal Center of the Jinling Hospital for 10 days before the experiment. The temperature was maintained at about 25 °C in both the breeding room and the operation room. All procedures were approved by the Animal Care and Use Committee of Nanjing University and conformed to the Guide for the Care and Use of Laboratory Animals by the National Institutes of Health.

4.2. Experimental Design

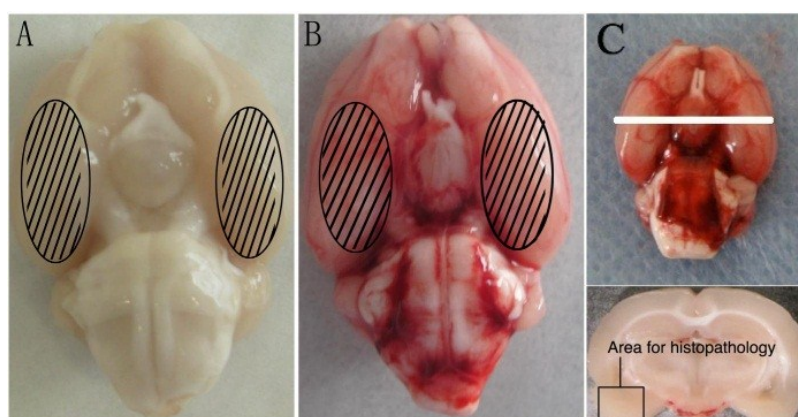
Ninety-six male SD rats were randomly divided into four groups: SAH group ($n = 24$); SAH + ATX group ($n = 24$); SAH + vehicle group ($n = 24$); and control group ($n = 24$). In the SAH + ATX group, ATX (20 μ L of 0.1 mM dissolved in vehicle) was administrated at 30 min after SAH was induced. Rats of the SAH + vehicle group received equal volumes of vehicles (20 μ L of 10% dimethylsulfoxide) at the corresponding time points. ATX or vehicle was administrated into the left ventricle (0.8 mm posterior, 1.5 mm lateral to the bregma, and 3.7 mm below dural) with a 25- μ L Hamilton syringe (Shanghai Gaoge Industry & Trade Co. Ltd., Shanghai, China). The dose of ATX was chosen according to our previous study since we observed beneficial effects on reducing oxidant damage in the SAH models [5]. Rats in each group were killed at 24 h after SAH (Figure 10).

Figure 10. Schematic illustration of experimental design.

4.3. Prechiasmatic Cistern SAH Model

The prechiasmatic cistern SAH model was produced according to a previous study under aseptic conditions [10]. The animal head was fixed in the stereotactic frame after the intraperitoneal anesthesia with pentobarbital sodium (50 mg/kg). A needle with a rounded tip and a side hole was tilted 45° in the sagittal plane and placed 7.5 mm anterior to bregma in the midline, with the hole facing the right side. It was advanced until the tip reached the skull base, about 2–3 mm anterior to the chiasma (10–12 mm away from the brain surface), and then retrieved 0.5 mm. Plugging the burr hole with bone wax prevented loss of cerebrospinal fluid and bleeding from the midline vessels. 0.25 ml non-heparinized fresh autologous arterial blood from the femoral artery was slowly injected into the prechiasmatic cistern for 20 s with a syringe pump. Animals in the control group were injected with 0.25 mL saline. The rats were sent back to their cages individually and received *ad libitum* access to food and water. Heart rate and rectal temperature were monitored, and the rectal temperature was kept at 37 °C ± 0.5 °C, using a warm pad if required. It was observed in the SAH models that the inferior basal temporal lobe was stained by blood (Figure 11).

Figure 11. Representative photographs of brains taken for detection. (A) Rat brain of the control group and (B) the subarachnoid hemorrhage (SAH) group acutely removed following saline perfusion; (A–C) The detected areas of the cortex sample for relative assays are schematized.



4.4. Immunohistochemistry

Six rats in each group were sacrificed for immunohistochemistry and terminal deoxynucleotidyl transferase-mediate dUTP nick end labeling (TUNEL) staining, using the fixation perfusion method as described [7,33]. The whole brain was removed and immersed in the fixative solution after perfusion-fixation. The formalin-fixed tissues were embedded in paraffin and cut to thickness sections (4 μ m) with a microtome. Immunohistochemistry was performed to determine the immunoreactivity of Nrf2 and HO-1. Briefly, sections were incubated at 4 °C overnight with primary antibody anti-Nrf2 (1:100; Abcam, Cambridge, MA, USA) and anti-HO-1 (1:200; Abcam, Cambridge, MA), then incubated with goat anti-rabbit horseradish peroxidase (HRP)-conjugated IgG (1:500, Santa Cruz Biotechnology, Santa Cruz, CA, USA) as secondary antibody. Sections were placed in an avidin-biotin-peroxidase complex enzyme after incubating. As following, 3,3'-diaminobenzidine (DAB) and hydrogen peroxide were used for staining.

4.5. TUNEL Assay

In situ cell death detection Kit POD (ISCDD, Boehringer Mannheim, Mannheim, Germany) was used for the TUNEL assay. The assay was performed according to the manufacturer's instructions and previous studies. Sections were deparaffinized, hydrated, and washed with distilled water. The tissues were digested with 20 g/mL proteinase K (Boehringer Mannheim, Mannheim, Germany) at room temperature for 15 min. Endogenous peroxidase activity was blocked by incubation in 0.3% hydrogen peroxide/methanol in phosphate buffered saline (PBS) at 37 °C for 30 min. The sections were incubated with terminal deoxynucleotidyl transferase at 37 °C for 60 min to add the dioxigenin-conjugated dUTP to the 3'-OH ends of fragmented DNA. Anti-dioxigenin antibody peroxidase was applied to the sections to detect the labeled nucleotides. After that, the sections were stained with DAB and counterstained slightly with hematoxylin.

4.6. Cell Counting

One slice of every six serial cuttings was selected, and altogether six slices were collected and observed in the light microscope by two independent investigators blinded to the experimental groups. The number of positive cells in each section was counted in 10 microscope fields (at $\times 200$ magnification) throughout the identical regions of the studied brain, and the mean per visual field was calculated.

4.7. Western Blot Analysis

The brain sample of rat was removed rapidly after saline perfusion and rinsed in 0.9% normal saline (4 °C) to wash away the blood and blood clot. And then the tissue was frozen in liquid nitrogen for molecular biological and biochemical experiments. The protein concentration was estimated by the Bradford method with the Nanjing Jiancheng protein assay kit (Nanjing Jiancheng Bioengineering Institute, Nanjing, China). The frozen sample was homogenized in 20 mM Tris (pH 7.6) which contains 0.2% SDS, 1% Triton X-100, 1% deoxycholate, 1 mM phenylmethylsulphonyl fluoride (PMSF), and 0.11 IU/mL aprotinin (all from Sigma-Aldrich, Inc., St. Luis, MO, USA) for HO-1 analysis. Lysate was centrifuged for 20 min (at 12,000 \times g, 4 °C), and the supernatant was collected. Nuclear protein was extracted for Nrf2 analysis as described [33,34]. Equal amount of protein per lane was separated by 10%

sodium dodecyl sulfate polyacrylamide gel electrophoresis (SDS-PAGE) and transferred to polyvinylidene-difluoride membrane (Bio-Rad Lab, Hercules, CA, USA). The membrane was blocked in 5% skimmed milk for 2 h at room temperature, and incubated overnight at 4 °C with primary antibodies against Nrf2 (1:1000, Abcam, Cambridge, MA, USA), HO-1 (1:2000, Abcam) and GAPDH (1:5000, Abcam) in PBS + Tween 20 (PBST) containing 1% skimmed milk. After the membrane was washed for 10 min each for four times in PBST, it was incubated with goat anti-rabbit HRP-conjugated IgG (diluted 1:1000 in phosphate-buffered saline/Tween (PBST), Abcam, Cambridge, UK) for two hours at room temperature. The blotted protein bands were visualized by enhanced chemiluminescence (ECL) Western blot detection reagents (Amersham, Arlington Heights, IL, USA) and were exposed to X-ray films. Developed films were digitized with an Epson Perfection 2480 scanner (Seiko Corp, Nagano, Japan). Optical densities were obtained using the UN-Scan-It 6.1 software (Silk Scientific Inc., Orem, UT, USA) and the data were normalized to β -actin.

4.8. Quantitative Real-Time PCR

Real-time PCR was used to analyze the mRNA levels of HO-1, NQO1 and GST- α 1. Total RNA from brain sample was extracted using Biomiga Tissue RNA Kit (Biomiga Inc., San Diego, CA, USA) following the manufacturer's instructions. Reverse transcription was performed using Promega (Madison, WI, USA) reagents. Real-time PCR analysis proceeded by real-time DNA analysis system (Genetimes Technology, Inc., Shanghai, China), using real-time SYBR Green PCR technology.

Forward and reverse primers were 5'-GCGAAACAAGCAGAACCCA-3' and 5'-GCTCAGGATGA GTACCTCCCA-3' for HO-1 (185 bp); 5'-GCGTCTGGAGACTGTCTGGG-3' and 5'-CGGCTGGAA TGGACTTGC-3' for NQO1 (170 bp); 5'-CGGTACTTGCCTGCCTTTG-3' and 5'-ATTTGTTTTGCA TCCACGGG-3' for GST- α 1 (248 bp); 5'-CCCATCTATGAGGGTTACGC-3' and 5'-TTTAATGTCA CGCACGATTTC-3' for β -actin (150 bp).

4.9. Enzyme Activity Assay

The frozen cortex tissue was homogenized in 10 mM Tris-HCl (pH 7.8) and centrifuged for 15 min (at 12000 \times g, 48 °C). The supernatant was collected, and NQO1 enzyme activity was measured by the reduction of the dicumarol-sensitive fraction of 2, 6-dichlorophenol-indo-phenol with spectrophotometry at 540 nm. GST- α 1 enzyme activity was determined by conjugation reaction of 1-chloro-2, 4-dinitrobenzene and glutathione, calculating slope elevation of extinction coefficient at 340 nm.

4.10. MDA Level Determination

The MDA level was determined using the method described in a previous study [5,35]. The MDA concentrations were measured as nanomoles/milligram. The principle of the MDA level assay depends on the lipid peroxidation products with thiobarbituric acid and formation of products called thiobarbituric acid-reacting substances, which give maximum absorbance at the 535 nm.

4.11. Brain Water Content

Rats were anesthetized and decapitated at 24 h after SAH. Brains were rapidly removed and immediately weighed as wet weight. Samples were subsequently placed in an oven for 72 h at 100 °C and weighed again to get the dry weight. The brain water content (%) was calculated as a percentage using the following method: $(\text{wet weight} - \text{dry weight})/\text{wet weight} \times 100\%$ [36].

4.12. Blood-Brain Barrier Permeability

BBB permeability was assessed by EB extravasation at 24 h after SAH. EB dye (2%; 4 mL/kg) was injected over two minutes into the right femoral vein to circulate for 60 min. Rats were then anaesthetized and perfused from the left cardiac ventricle to the right cardiac atrium with normal saline to replace the EB dye. The brains were removed after the decapitations and then homogenized in phosphate-buffered saline. Trichloroacetic acid was added to deposit the protein. After that, samples were cooled and centrifuged. The supernatant was dislodged to measure absorbance of EB at 620 nm by a spectrophotometer (752S UV-Vis Spectrophotometer, Lengguang Tech., Shanghai, China).

4.13. Statistical Analysis

All data were presented as mean \pm SEM. SPSS 20.0 was used for statistical analysis of the data. Kruskal-Wallis test followed by the Dunnis *post hoc* test were used to compare the differences among groups for neurological scores. The other data were subjected to one-way ANOVA and Tukey's multiple comparison test. Differences with $p < 0.05$ were considered statistically significant.

5. Conclusions

In summary, to the best of our knowledge, this study was the first one to demonstrate the effects of ATX on the Nrf2-ARE pathway in the cerebral cortex after SAH. The results of the present study suggest that ATX treatment 30 min after SAH can result in further activation of the Nrf2-ARE pathway and, accordingly, ameliorate EBI after SAH. The benefit of ATX treatment might be caused by the up-regulation of Nrf2 trans-activating enzymes to suppress oxidative damage, which was one of its potential mechanisms. These findings are novel for the therapeutic strategy of EBI after SAH.

Acknowledgments

This work was supported by grants from the National Natural Science Foundation of China (NSFC): No. 81471183 (X Zhang), the Natural Science Foundation of Jiangsu Province: No. BK2014377 (X Zhang) and the special funds from Clinical Medicine Research of Jiangsu Province: No. BL2013027 (HD Wang).

Author Contributions

Qi Wu, Xiang-Sheng Zhang, Qing Yu, Wei Li, Meng-Liang Zhou and Xiao-liang Wang participated in the experimental procedures. Qi Wu, Xin Zhang, and Han-dong Wang participated in the design of the study and the writing of the manuscript. All authors read and approved the final manuscript.

Conflicts of Interest

The authors declare no conflict of interest.

References

1. Tripathi, D.N.; Jena, G.B. Astaxanthin intervention ameliorates cyclophosphamide-induced oxidative stress, DNA damage and early hepatocarcinogenesis in rat: Role of Nrf2, p53, p38 and phase-II enzymes. *Mutat. Res.* **2010**, *696*, 69–80.
2. Shen, H.; Kuo, C.C.; Chou, J.; Delvolve, A.; Jackson, S.N.; Post, J.; Woods, A.S.; Hoffer, B.J.; Wang, Y.; Harvey, B.K. Astaxanthin reduces ischemic brain injury in adult rats. *FASEB J.* **2009**, *23*, 1958–1968.
3. Liu, X.; Shibata, T.; Hisaka, S.; Osawa, T. Astaxanthin inhibits reactive oxygen species-mediated cellular toxicity in dopaminergic SH-SY5Y cells via mitochondria-targeted protective mechanism. *Brain Res.* **2009**, *1254*, 18–27.
4. Ikeda, Y.; Tsuji, S.; Satoh, A.; Ishikura, M.; Shirasawa, T.; Shimizu, T. Protective effects of astaxanthin on 6-hydroxydopamine-induced apoptosis in human neuroblastoma SH-SY5Y cells. *J. Neurochem.* **2008**, *107*, 1730–1740.
5. Zhang, X.S.; Zhang, X.; Zhou, M.L.; Zhou, X.M.; Li, N.; Li, W.; Cong, Z.X.; Sun, Q.; Zhuang, Z.; Wang, C.X.; *et al.* Amelioration of oxidative stress and protection against early brain injury by astaxanthin after experimental subarachnoid hemorrhage. *J. Neurosurg.* **2014**, *121*, 42–54.
6. Pluta, R.M.; Hansen-Schwartz, J.; Dreier, J.; Vajkoczy, P.; Macdonald, R.L.; Nishizawa, S.; Kasuya, H.; Wellman, G.; Keller, E.; Zauner, A.; *et al.* Cerebral vasospasm following subarachnoid hemorrhage: Time for a new world of thought. *Neurol. Res.* **2009**, *31*, 151–158.
7. Zhao, X.D.; Zhou, Y.T.; Zhang, X.; Wang, X.L.; Qi, W.; Zhuang, Z.; Su, X.F.; Shi, J.X. Expression of NF-E2-related factor 2 (Nrf2) in the basilar artery after experimental subarachnoid hemorrhage in rabbits: A preliminary study. *Brain Res.* **2010**, *1358*, 221–227.
8. Jin, W.; Wang, H.; Ji, Y.; Hu, Q.; Yan, W.; Chen, G.; Yin, H. Increased intestinal inflammatory response and gut barrier dysfunction in Nrf2-deficient mice after traumatic brain injury. *Cytokine* **2008**, *44*, 135–140.
9. Yang, C.; Zhang, X.; Fan, H.; Liu, Y. Curcumin upregulates transcription factor Nrf2, HO-1 expression and protects rat brains against focal ischemia. *Brain Res.* **2009**, *1282*, 133–141.
10. Chen, G.; Fang, Q.; Zhang, J.; Zhou, D.; Wang, Z. Role of the Nrf2-ARE pathway in early brain injury after experimental subarachnoid hemorrhage. *J. Neurosci. Res.* **2011**, *89*, 515–523.
11. Zhang, X.; Zhao, W.E.; Hu, L.; Zhao, L.; Huang, J. Carotenoids inhibit proliferation and regulate expression of peroxisome proliferators-activated receptor gamma (PPARgamma) in K562 cancer cells. *Arch. Biochem. Biophys.* **2011**, *512*, 96–106.
12. Wang, Z.; Ma, C.; Meng, C.J.; Zhu, G.Q.; Sun, X.B.; Huo, L.; Zhang, J.; Liu, H.X.; He, W.C.; Shen, X.M.; *et al.* Melatonin activates the Nrf2-ARE pathway when it protects against early brain injury in a subarachnoid hemorrhage model. *J. Pineal Res.* **2012**, *53*, 129–137.

13. Claassen, J.; Carhuapoma, J.R.; Kreiter, K.T.; Du, E.Y.; Connolly, E.S.; Mayer, S.A. Global cerebral edema after subarachnoid hemorrhage: frequency, predictors, and impact on outcome. *Stroke* **2002**, *33*, 1225–1232.
14. Cahill, J.; Zhang, J.H. Subarachnoid hemorrhage: Is it time for a new direction? *Stroke* **2009**, *40*, S86–S87.
15. Ayer, R.E.; Zhang, J.H. Oxidative stress in subarachnoid haemorrhage: Significance in acute brain injury and vasospasm. *Acta Neurochir. Suppl.* **2008**, *104*, 33–41.
16. Ostrowski, R.P.; Colohan, A.R.; Zhang, J.H. Molecular mechanisms of early brain injury after subarachnoid hemorrhage. *Neurol. Res.* **2006**, *28*, 399–414.
17. Ye, Q.; Huang, B.; Zhang, X.; Zhu, Y.; Chen, X. Astaxanthin protects against MPP(+)-induced oxidative stress in PC12 cells via the HO-1/NOX2 axis. *BMC Neurosci.* **2012**, *13*, 156.
18. Chan, K.C.; Mong, M.C.; Yin, M.C. Antioxidative and anti-inflammatory neuroprotective effects of astaxanthin and canthaxanthin in nerve growth factor differentiated PC12 cells. *J. Food Sci.* **2009**, *74*, H225–H231.
19. Fassett, R.G.; Coombes, J.S. Astaxanthin, oxidative stress, inflammation and cardiovascular disease. *Future Cardiol.* **2009**, *5*, 333–342.
20. Lauver, D.A.; Lockwood, S.F.; Lucchesi, B.R. Disodium Disuccinate Astaxanthin (Cardax) attenuates complement activation and reduces myocardial injury following ischemia/reperfusion. *J. Pharmacol. Exp. Ther.* **2005**, *314*, 686–692.
21. Gross, G.J.; Lockwood, S.F. Cardioprotection and myocardial salvage by a disodium disuccinate astaxanthin derivative (Cardax). *Life Sci.* **2004**, *75*, 215–224.
22. Pan, H.; Wang, H.; Zhu, L.; Mao, L.; Qiao, L.; Su, X. Depletion of Nrf2 enhances inflammation induced by oxyhemoglobin in cultured mice astrocytes. *Neurochem. Res.* **2011**, *36*, 2434–2441.
23. Van Muiswinkel, F.L.; Kuiperij, H.B. The Nrf2-ARE Signalling pathway: Promising drug target to combat oxidative stress in neurodegenerative disorders. *Curr. Drug Targets CNS Neurol. Disord.* **2005**, *4*, 267–281.
24. Ben-Dor, A.; Steiner, M.; Gheber, L.; Danilenko, M.; Dubi, N.; Linnewiel, K.; Zick, A.; Sharoni, Y.; Levy, J. Carotenoids activate the antioxidant response element transcription system. *Mol. Cancer Ther.* **2005**, *4*, 177–186.
25. Radjendirane, V.; Joseph, P.; Lee, Y.H.; Kimura, S.; Klein-Szanto, A.J.; Gonzalez, F.J.; Jaiswal, A.K. Disruption of the DT diaphorase (NQO1) gene in mice leads to increased menadione toxicity. *J. Biol. Chem.* **1998**, *273*, 7382–7389.
26. Shih, A.Y.; Johnson, D.A.; Wong, G.; Kraft, A.D.; Jiang, L.; Erb, H.; Johnson, J.A.; Murphy, T.H. Coordinate regulation of glutathione biosynthesis and release by Nrf2-expressing glia potently protects neurons from oxidative stress. *J. Neurosci.* **2003**, *23*, 3394–3406.
27. Ku, B.M.; Joo, Y.; Mun, J.; Roh, G.S.; Kang, S.S.; Cho, G.J.; Choi, W.S.; Kim, H.J. Heme oxygenase protects hippocampal neurons from ethanol-induced neurotoxicity. *Neurosci. Lett.* **2006**, *405*, 168–171.
28. Zipper, L.M.; Mulcahy, R.T. Erk activation is required for Nrf2 nuclear localization during pyrrolidine dithiocarbamate induction of glutamate cysteine ligase modulatory gene expression in HepG2 cells. *Toxicol. Sci.* **2003**, *73*, 124–134.

29. Wang, H.Q.; Sun, X.B.; Xu, Y.X.; Zhao, H.; Zhu, Q.Y.; Zhu, C.Q. Astaxanthin upregulates heme oxygenase-1 expression through ERK1/2 pathway and its protective effect against beta-amyloid-induced cytotoxicity in SH-SY5Y cells. *Brain Res.* **2010**, *1360*, 159–167.
30. Kim, J.H.; Nam, S.W.; Kim, B.W.; Kim, W.J.; Choi, Y.H. Astaxanthin improves the proliferative capacity as well as the osteogenic and adipogenic differentiation potential in neural stem cells. *Food Chem. Toxicol.* **2010**, *48*, 1741–1745.
31. Prunell, G.F.; Mathiesen, T.; Svendgaard, N.A. A new experimental model in rats for study of the pathophysiology of subarachnoid hemorrhage. *Neuroreport* **2002**, *13*, 2553–2556.
32. Prunell, G.F.; Mathiesen, T.; Svendgaard, N.A. Experimental subarachnoid hemorrhage: Cerebral blood flow and brain metabolism during the acute phase in three different models in the rat. *Neurosurgery* **2004**, *54*, 426–436.
33. Yan, W.; Wang, H.D.; Zhu, L.; Feng, X.M.; Qiao, L.; Jin, W.; Tang, K. Traumatic brain injury induces the activation of the Nrf2-ARE pathway in the lung in rats. *Brain Injury* **2008**, *22*, 802–810.
34. Yan, W.; Wang, H.D.; Feng, X.M.; Ding, Y.S.; Jin, W.; Tang, K. The expression of NF-E2-related factor 2 in the rat brain after traumatic brain injury. *J. Trauma* **2009**, *66*, 1431–1435.
35. Fang, Q.; Chen, G.; Zhu, W.; Dong, W.; Wang, Z. Influence of melatonin on cerebrovascular proinflammatory mediators expression and oxidative stress following subarachnoid hemorrhage in rabbits. *Mediat. Inflamm.* **2009**, *2009*, 426346.
36. Jin, W.; Wang, H.; Yan, W.; Zhu, L.; Hu, Z.; Ding, Y.; Tang, K. Role of Nrf2 in protection against traumatic brain injury in mice. *J. Neurotrauma* **2009**, *26*, 131–139.

© 2014 by the authors; licensee MDPI, Basel, Switzerland. This article is an open access article distributed under the terms and conditions of the Creative Commons Attribution license (<http://creativecommons.org/licenses/by/4.0/>).